

Long range order and two-fluid behavior in heavy electron materials

K. R. Shirer ^{*}, A. C. Shockley ^{*}, A. P. Dioguardi ^{*}, J. Crocker ^{*}, C.-H. Lin ^{*}, N. apRoberts-Warren ^{*}, D. M. Nisson ^{*}, P. Klavins ^{*}, J. C. Cooley [†], Y.-F. Yang [‡] and N. J. Curro ^{*}

^{*}Department of Physics, University of California, Davis, CA 95616, USA, [†]Los Alamos National Laboratory, Los Alamos, New Mexico 87545, USA, and [‡]Beijing National Laboratory for Condensed Matter Physics and Institute of Physics, Chinese Academy of Sciences, Beijing 100190 China

Submitted to Proceedings of the National Academy of Sciences of the United States of America

The heavy electron Kondo liquid is an emergent state of condensed matter that displays universal behavior independent of material details. Properties of the heavy electron liquid are best probed by NMR Knight shift measurements, which provide a direct measure of the behavior of the heavy electron liquid that emerges below the Kondo lattice coherence temperature as the lattice of local moments hybridizes with the background conduction electrons. Because the transfer of spectral weight between the localized and itinerant electronic degrees of freedom is gradual, the Kondo liquid typically co-exists with the local moment component until the material orders at low temperatures. The two-fluid formula captures this behavior in a broad range of materials in the paramagnetic state. In order to investigate two-fluid behavior and the onset and physical origin of different long range ordered ground states in heavy electron materials, we have extended Knight shift measurements to URu₂Si₂, CeRhIn₅ and CeRhIn₅. In CeRhIn₅ we find that the antiferromagnetic order is preceded by a relocalization of the Kondo liquid, providing independent evidence for a local moment origin of antiferromagnetism. In URu₂Si₂ the hidden order is shown to emerge directly from the Kondo liquid and so is not associated with local moment physics. Our results imply that the nature of the ground state is strongly coupled with the hybridization in the Kondo lattice in agreement with phase diagram proposed by Yang and Pines.

Heavy Fermion | NMR | Hidden Order | Antiferromagnetism

Competition between different energy scales gives rise to a rich spectrum of emergent ground states in strongly correlated electron materials. In the heavy fermion compounds, a lattice of nearly localized f-electrons interacts with a sea of conduction electrons, and depending on the magnitude of this interaction different types of long range order may develop at low temperatures [1]. The Kondo lattice model strives to capture the essential physics of heavy fermion materials by considering the various magnetic interactions between the conduction electron spins, S_c , and the local moment spins, S_f [2]. Different ground states can emerge depending on the relative strengths of the interaction, J , between S_c and S_f and the intersite interaction, J_{ff} , between the S_f spins [3, 4]. Much of the physics of the phase diagram is driven by a quantum critical point, which separates long-range ordered ground states from those in which the local moments have fully hybridized with the conduction electrons to form itinerant states with large effective masses and large Fermi surfaces [5]. In several materials quantum critical fluctuations give rise to anomalous non-Fermi liquid behavior in various bulk transport and thermodynamic quantities [6, 7, 8].

In recent years, evidence has emerged that in the high temperature disordered phase the electronic degrees of freedom simultaneously exhibit both itinerant and localized behavior [9]. Below a temperature T^* that marks the onset of hybridization or lattice coherence, several experimental quantities exhibit a temperature dependence that is well described by a fluid of hybridized heavy quasiparticles coexisting with partially screened local moments [3, 10]. In the two fluid picture, the transfer of spectral weight from the local moments to the heavy electrons is described by a quantity $f(T)$ [10]. Above a

temperature T^* , the local moments and conduction electrons remain uncoupled. Below T^* the local moments gradually dissolve into the hybridized heavy electron fluid as the temperature is lowered. This crossover can be measured directly via nuclear magnetic resonance (NMR) Knight shift experiments [11]. The contribution to the Knight shift from the heavy electrons, K_{HF} , exhibits a universal logarithmic divergence with decreasing temperature below T^* in the paramagnetic state. In superconducting CeCoIn₅ this scaling persists down to T_c indicating that the condensate emerges from the heavy electron degrees of freedom [12]. Relatively little is known, however, about how this scaling behaves in materials with other types of ordered ground states. Here we report Knight shift data in both URu₂Si₂ and CeRhIn₅. In the former the scaling persists down to the onset of hidden order at T_{HO} ; but in the latter the heavy electron spectral weight reverses course and the local moments relocalize above the Neel temperature, T_N , similar to the antiferromagnet CePt₂In₇ [13]. These results imply generally that the heavy electron fluid is either unstable to a Fermi surface instability such as hidden order or superconductivity, or collapses to form ordered local moments.

Knight Shift anomalies

The Zeeman interaction of an isolated nuclear spin $\hat{\mathbf{I}}$ in an external magnetic field \mathbf{H}_0 is given by $\mathcal{H}_Z = \gamma\hbar\hat{\mathbf{I}} \cdot \mathbf{H}_0$, where γ is the gyromagnetic ratio and \hbar is the reduced Planck constant. In this case the nuclear spin resonance frequency is given by the Larmor frequency $\omega_L = \gamma H_0$. In condensed matter systems the nuclear spins typically experience a hyperfine coupling to the electron spins, $\mathcal{H}_{hyp} = \gamma\hbar g\mu_B\hat{\mathbf{I}} \cdot \mathbf{A} \cdot \mathbf{S}$, where \mathbf{S} is the electron spin and \mathbf{A} is the hyperfine coupling. The hyperfine coupling is in general a tensor that depends on the details of the bonding and quantum chemistry of the material of interest. \mathbf{S} can be the unpaired spin moment of an unfilled shell, the net conduction electron spin of a Fermi sea polarized by a magnetic field, or the spin-orbit coupled moment of a localized electron. \mathbf{S} may or may not be located on the same ion as the nuclear moment; the former is referred to as *on-site* coupling and the latter is *transferred* coupling. In the paramagnetic state the electron spin is polarized by the external

Reserved for Publication Footnotes

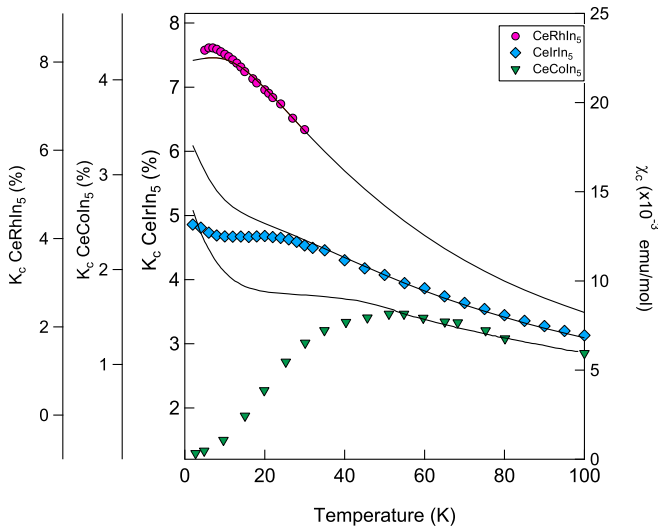


Fig. 1. The Knight shift (solid points) and the bulk susceptibility (solid lines) of the $\text{In}(1)$ for field along the c -direction in CeMIn_5 for $\text{M} = \text{Rh}, \text{Ir}$ and Co . T^* is the temperature where the two quantities no longer are proportional to one another, and is clearly material dependent. In some cases K appears to exceed χ and in others K decreases.

field $\mathbf{S} = \chi \cdot \mathbf{H}_0 / g\mu_B$, where χ is the susceptibility. Thus the nuclear spin experiences an effective Hamiltonian:

$$\mathcal{H}_Z + \mathcal{H}_{hyp} = \gamma \hbar \hat{\mathbf{I}} \cdot (\mathbf{1} + \mathbf{K}) \cdot \mathbf{H}_0, \quad [1]$$

where the Knight shift tensor $\mathbf{K} = \mathbf{A} \cdot \chi$ is unit-less. The resonance frequency is given by $\omega = \omega_L(1 + K(\theta, \phi))$, where $K(\theta, \phi) = \mathbf{H}_0 \cdot \mathbf{A} \cdot \chi \cdot \mathbf{H}_0 / H_0^2$ depends on the polar angles θ and ϕ that describe the relative orientation of the field with respect to the principal axes of the Knight shift tensor. For the isotropic case the shift $K = A\chi$ is independent of direction. Strictly speaking the *Knight* shift was originally defined as the paramagnetic shift from the Pauli susceptibility

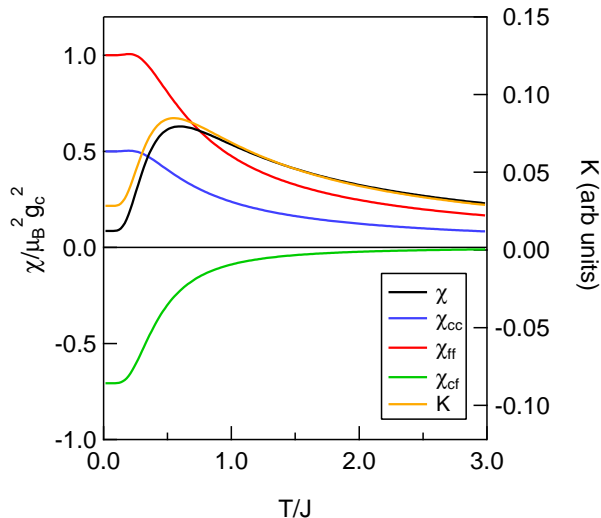


Fig. 2. The components of the magnetic susceptibility for the model spin system. The Knight shift begins to deviate from the bulk susceptibility below a temperature $T \approx J$. In this case, we have used $g_f/g_c = \sqrt{2}$, and $B/A = 1.5$. If $g_f = g_c$, then $\chi(T \rightarrow 0) \rightarrow 0$, as expected for a singlet ground state.

in metals, but in practice refers to any shift K arising from the electronic susceptibility.

The magnetic susceptibility and the Knight shift can be measured independently. One can extract the hyperfine coupling A by plotting the Knight shift versus the susceptibility with temperature as an implicit parameter (such a plot is traditionally known as a *Clogston-Jaccarino* plot [14]). If there is a single electronic spin component that gives rise to the magnetic susceptibility, then the Clogston-Jaccarino plot is a straight line with slope A and intercept K_0 . K_0 is a temperature independent offset that is usually given by the orbital susceptibility and diamagnetic contributions [15].

Breakdown of linearity and failure of local pictures. All known heavy fermion materials exhibit a Knight shift anomaly where the Clogston-Jaccarino plot deviates from linearity below an onset temperature, T^* [11]. This phenomenon is also visible in a plot comparing K and χ versus temperature, as seen in Fig. 1, where T^* marks the temperature below which K no longer tracks χ . This breakdown can arise from the presence of impurity phases, which contribute to the bulk susceptibility but not to the Knight shift. However Knight shift anomalies occur ubiquitously in single phase highly pure heavy fermion

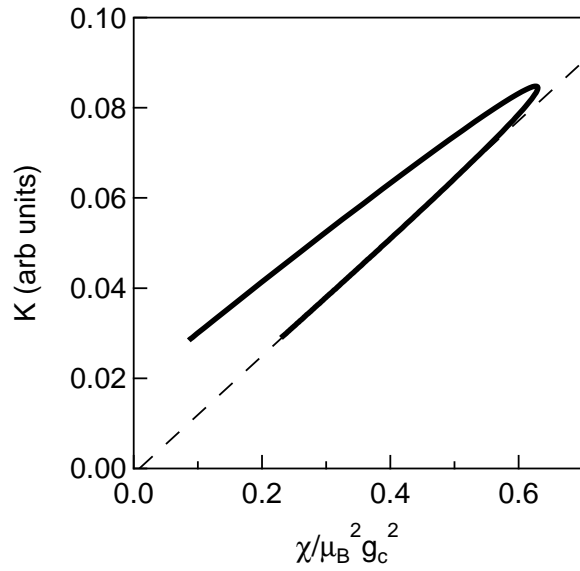


Fig. 3. Knight shift versus the bulk susceptibility for the model spin system with temperature as an implicit parameter. The Knight shift begins to deviate from the bulk susceptibility below a temperature $T \approx J/k_B$. In this case, we have used $g_f/g_c = \sqrt{2}$, and $B/A = 1.5$.

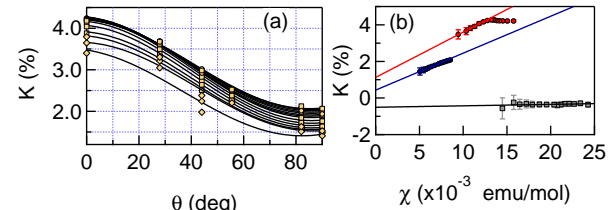


Fig. 4. (a) The Knight shift of the $\text{In}(1)$ in CeIrIn_5 versus angle at several different temperatures. Solid points are fits to Eq. 4. (b) K_{aa} (blue), K_{cc} (red) and K_{ac} (gray) versus χ_{aa} , χ_{cc} and $\chi_{aa} + \chi_{cc}$. Solid lines are linear fits as described in the text.

materials and are intrinsic phenomena. Several different theories have been proposed to explain these anomalies. These theories generally fall into two categories: (i) a temperature dependent hyperfine coupling $A(T)$, or (ii) multiple spin degrees of freedom. It has been argued that A acquires a temperature dependence either because of Kondo screening [16] or because of different populations of crystal field levels of the 4f(5f) electrons in these materials [17]. A major flaw in such an argument is that the hyperfine coupling is determined by large energy scales involving exchange integrals between different atomic orbitals, and since the Kondo and/or crystal field interactions are several orders of magnitude smaller they cannot give rise to large perturbations in the hyperfine couplings [18]. Furthermore, in materials such as the CeMIn₅ system both the Knight shift anomaly and the crystalline electric field interaction are well characterized and are clearly uncorrelated (see Table 1) [19].

Two spin components. Since Kondo lattice materials have both localized f-electrons and itinerant conduction electrons, a theory which includes different hyperfine couplings to multiple spin degrees of freedom fits better. The two-fluid picture correctly predicts the temperature dependence of the Knight shift anomalies seen experimentally in heavy fermion materials. In the Kondo lattice model the local moment spins, \mathbf{S}_f interact with a sea of conduction electron spins, \mathbf{S}_c through a Kondo interaction:

$$\mathcal{H}_K = J \sum_i \mathbf{S}_f(\mathbf{r}_i) \cdot \mathbf{S}_c + \sum_{ij} J_{ff}(\mathbf{r}_{ij}) \mathbf{S}_f(\mathbf{r}_i) \cdot \mathbf{S}_f(\mathbf{r}_j) \quad [2]$$

where the sums are over the lattice positions \mathbf{r}_i of the localized f electrons. The general solution of the Kondo lattice has not been resolved to date, but the two-fluid description given by Nakatsuji, Fisk, Pines and Yang provides a phenomenological framework to describe the phase diagram of the Kondo lattice problem [3, 4, 9, 10]. This approach offers a natural interpretation of the NMR Knight shift anomaly in terms of two hyperfine couplings to the two different electron spins:

$$\mathcal{H}_{hyp} = \gamma \hbar g \mu_B \hat{\mathbf{I}} \cdot (A \mathbf{S}_c + B \mathbf{S}_f) \quad [3]$$

where A and B are the hyperfine couplings to the conduction electron and local moment spins, respectively [11]. The sus-

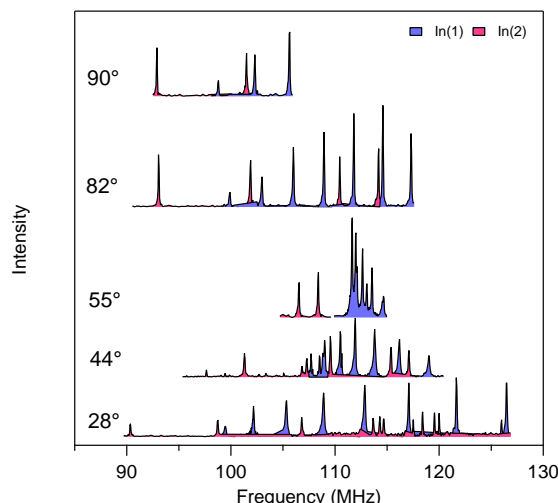


Fig. 5. Spectra of the In(1) and In(2) in CeIn₅ at 6 K and constant field of 11.7 T, where θ is the angle between the c axis and the field. There are multiple satellite transitions for each site due to the quadrupolar splitting [20].

ceptibility is the sum of three contributions $\chi = \chi_{cc} + 2\chi_{cf} + \chi_{ff}$, where $\chi_{\alpha\beta} = \langle \mathbf{S}_\alpha \mathbf{S}_\beta \rangle$ with $\alpha, \beta = c, f$. In the paramagnetic state $\langle S_c \rangle = (\chi_{cc} + \chi_{cf}) H_0$ and $\langle S_f \rangle = (\chi_{ff} + \chi_{cf}) H_0$, thus the Knight shift is given by:

$$K = K_0 + A\chi_{cc} + (A + B)\chi_{cf} + B\chi_{ff}. \quad [4]$$

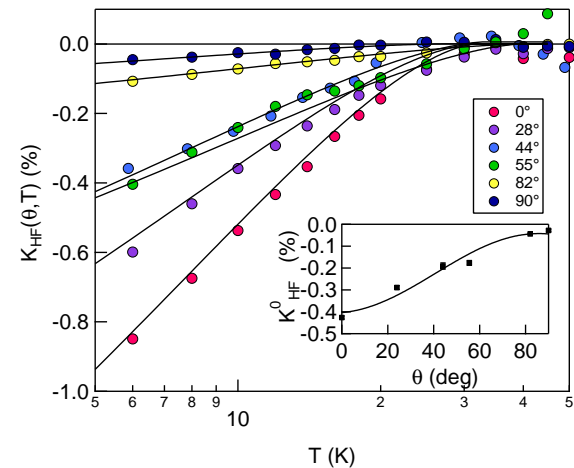


Fig. 6. The heavy electron component of the shift in CeIn₅ for the In(1) as a function of angle and temperature. The solid lines are fits to Eq. 9. Inset: The fitted value K_{HF}^0 versus angle. The solid line fit, described in the text, indicates the tensor nature of the hyperfine coupling \mathbf{A} .

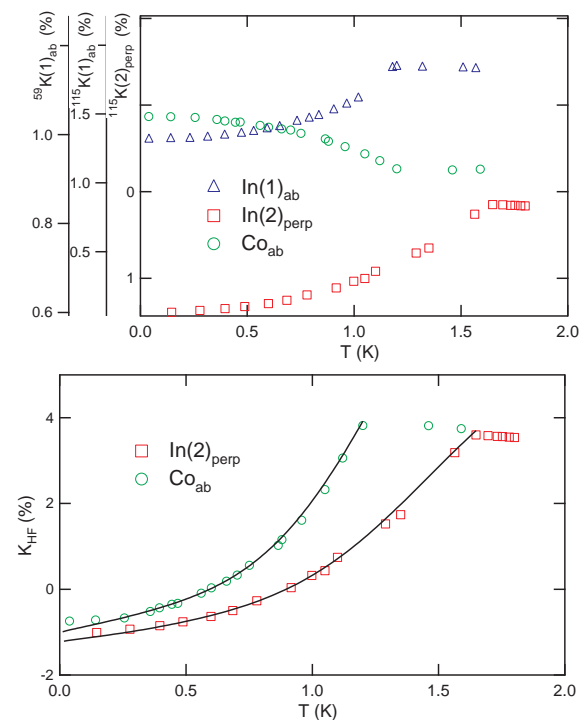


Fig. 7. (upper panel) Knight shift of the In(1), In(2) and Co in CeCoIn₅ in the paramagnetic state for field in the ab plane. For In(2) there are two distinct crystallographic positions depending on the direction of the field. (lower panel) The heavy electron susceptibility K_{HF} in the superconducting state. The solid lines are calculations as discussed in the text. Data are reproduced from [12].

The Knight shift weighs the different correlation functions separately than the total susceptibility, which leads to important consequences if the correlation functions have different temperature dependences. $K \sim \chi$ if and only if $A = B$. If $A \neq B$, then the Clogston-Jaccarino plot will no longer be linear. By measuring K and χ independently, one can exploit this difference to extract linear combinations of these individual susceptibilities. No other experimental technique can access these susceptibilities.

Free spin model. The general solution for the susceptibilities $\chi_{\alpha\beta}$ of the Kondo lattice problem has not been solved to date. It is useful, however, to consider a simplified model. Consider

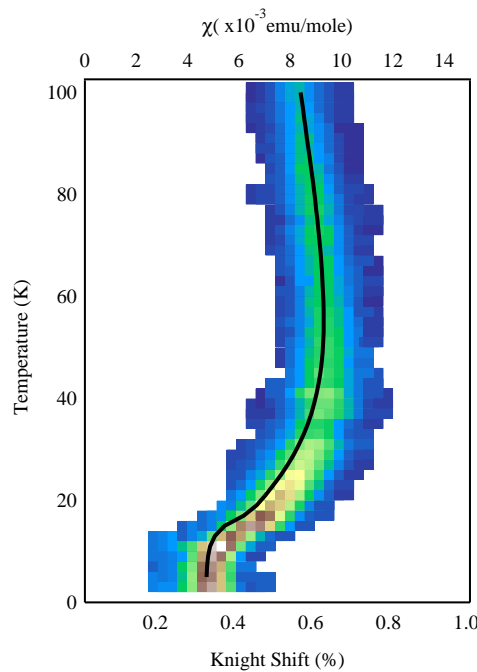


Fig. 8. Spectra of the ^{29}Si in URu_2Si_2 as a function of temperature. Color intensity (arb units) corresponds to the integral of the NMR spin echo. The solid black line is the bulk susceptibility.

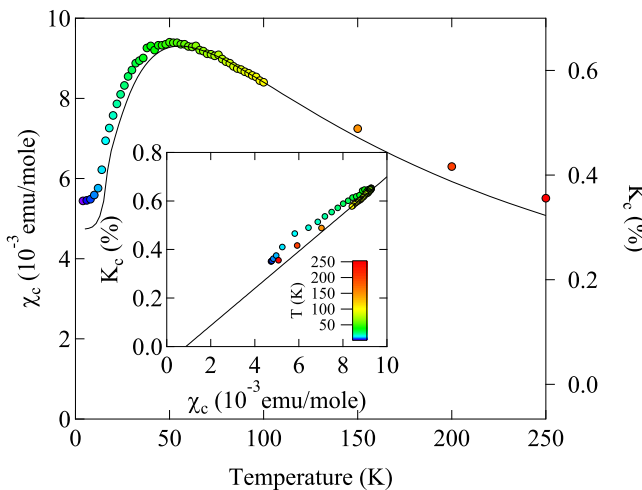


Fig. 9. The Knight shift of the Si (colored circles) and the susceptibility (solid line) in URu_2Si_2 for field along the c direction. The inset shows K versus χ_c .

the case of two free $S = \frac{1}{2}$ spins \mathbf{S}_c and \mathbf{S}_f that experience a Heisenberg coupling J . The Hamiltonian for this spin system in the presence of an external magnetic field \mathbf{H}_0 is given by:

$$\hat{\mathcal{H}} = g_c \mu_B \mathbf{S}_c \cdot \mathbf{H}_0 + g_f \mu_B \mathbf{S}_f \cdot \mathbf{H}_0 + J \mathbf{S}_c \cdot \mathbf{S}_f, \quad [5]$$

where μ_B is the Bohr magneton, and $g_{c,f}$ are the g-factors of the two different spins. This simplified model is clearly an *incorrect* physical description of the Kondo lattice problem where the spins are not free but part of a complex many-body problem involving the Fermi sea and various intersite interactions. This model is the simplest case, which captures the essence of the Knight shift anomaly and can be solved exactly.

The free energy is given by $F = -k_B T \ln Z$, where Z is the partition function; the susceptibility of the system is given by the second derivative of the free energy with respect to field: $\chi = \frac{\partial^2 F}{\partial H^2}|_{H \rightarrow 0}$. The exact susceptibility is given as the sum of three contributions:

$$\chi_{cc}(x) = \left(\frac{g_c^2 \mu_B^2}{4k_B T} \right) \frac{2(e^x + x - 1)}{(3 + e^x)x} \quad [6]$$

$$\chi_{ff}(x) = \left(\frac{g_f^2 \mu_B^2}{4k_B T} \right) \frac{2(e^x + x - 1)}{(3 + e^x)x} \quad [7]$$

$$\chi_{cf}(x) = -\left(\frac{g_c g_f \mu_B^2}{4k_B J} \right) \frac{2(e^x - x - 1)}{3 + e^x} \quad [8]$$

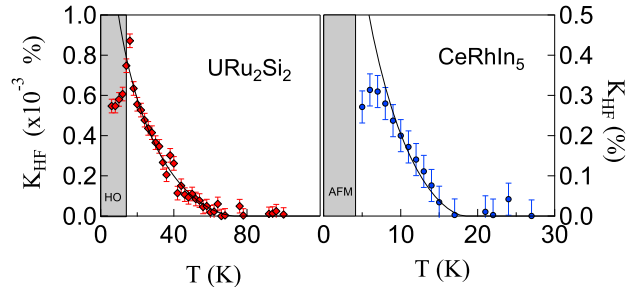


Fig. 10. $K_{HF}(T)$ versus T for URu_2Si_2 (left) and CeRhIn_5 (right). The solid black line are best fits to Eq. 9. In URu_2Si_2 K_{HF} grows until the sudden onset of hidden order, whereas in CeRhIn_5 K_{HF} deviates from the scaling form below 8 K indicating the relocalization of the local moments.

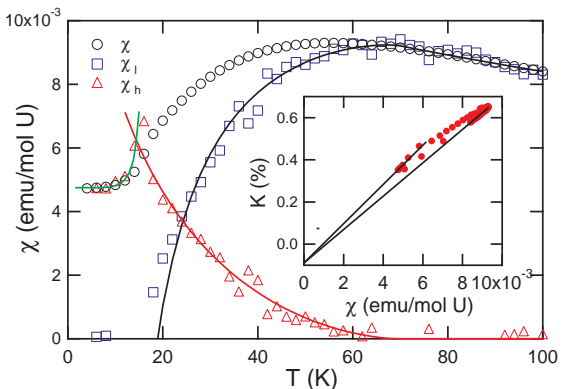


Fig. 11. Two-fluid analysis of the magnetic susceptibility in URu_2Si_2 by using the one-component behavior above T^* and below T_L . The solid lines are fit to the scaling formula of the Kondo liquid and the mean-field formula of the hybridized spin liquid for $T > T_{HO}$ and the Yosida function for $T < T_{HO}$ following the BCS prediction.

where $x = J/k_B T$. The temperature dependence of these three susceptibilities is shown in Fig. 2. In the high temperature limit ($T \gg J/k_B$) χ_{cc} and χ_{ff} exhibit Curie behavior and $\chi_{cf} \rightarrow 0$ as expected. For low temperature ($T \lesssim J/k_B$) the behavior is modified by the tendency to form a singlet ground state. As shown in Fig. 2 χ_{cc} , χ_{ff} and χ_{cf} change dramatically below $T \approx J/k_B$ and saturate at low temperatures. The Knight shift, given by Eq. 4, is shown as well in Fig. 2. Clearly K tracks χ for $T \gg J/k_B$ but deviates below $T \approx J/k_B$, creating an anomaly in the Clogston-Jaccarino plot in Fig. 3. The breakdown of linearity arises because $|\chi_{cf}|$ increases below $T \approx J/k_B$ and has a *different temperature dependence* than χ_{cc} and χ_{ff} .

Two-fluid model. The three individual susceptibilities $\chi_{\alpha\beta}$ will exhibit different temperature dependences in a Kondo lattice than the free spin model considered above. In particular, at high temperatures χ_{cc} is given by the temperature independent Pauli susceptibility of the conduction electrons, and χ_{ff} is given by a Curie-Weiss susceptibility of the local moments. Therefore above a crossover temperature, T^* , χ_{ff} dominates and $K = K_0 + B\chi$. Below T^* χ_{cf} becomes significant and the growth of this component can be measured by the quantity $K_{HF} = K - K_0 - B\chi = (A - B)(\chi_{cf} + \chi_{cc})$. The two-fluid model postulates that K_{HF} is proportional to the susceptibility of the heavy electron fluid; its temperature dependence probes both growth of hybridization and its relative spectral weight [3, 10]. Empirically it has been found that in the paramagnetic phase of a broad range of materials, $K_{HF}(T)$ varies as:

$$K_{HF}(T) = K_{HF}^0(1 - T/T^*)^{3/2}[1 + \log(T^*/T)] \quad [9]$$

where K_{HF}^0 is a constant [10]. In other words, K_{HF} exhibits a universal scaling with the quantity T/T^* , where T^* and K_{HF}^0 are material dependent quantities. K_{HF}^0 is proportional to $A - B$ and can be either positive or negative. T^* agrees well with several other experimental measurements of the coherence temperature of the Kondo lattice [10]. The Knight shift thus provides a direct probe of the susceptibility of the emergent heavy electron fluid in the paramagnetic state. There are, however, several pieces of missing information regarding the behavior of the heavy electron component that need to be

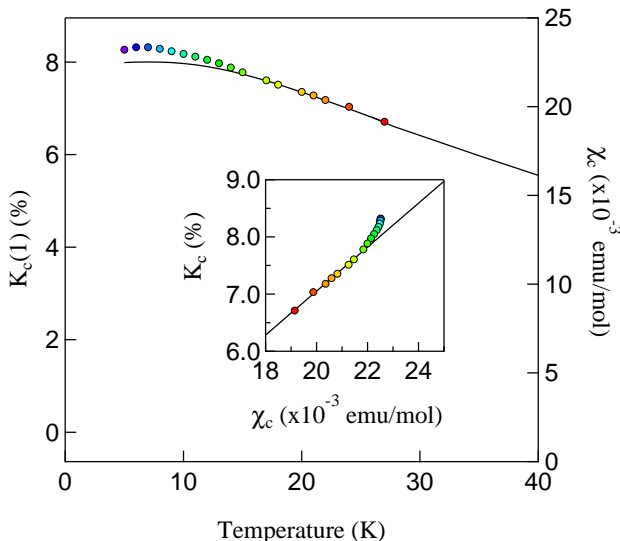


Fig. 12. The Knight shift of the In(1) (colored circles) and the susceptibility (solid line) in CeRhIn₅ for field along the c direction. The inset shows K versus χ .

addressed. For example, the Knight shift anomaly is strongly anisotropic in some materials, and is not been clear whether this is an intrinsic feature of the heavy electron fluid or rather a reflection of the anisotropy of the hyperfine couplings [11]. Furthermore, the Yang-Pines scaling works remarkably well for temperatures down to $\sim 10\%$ of T^* , but until recently there has been relatively little information about the evolution of the heavy electron fluid at lower temperature particularly when long-range order develops. We address both of these issues in turn below.

Anisotropy. One of the striking features of the emergence of the heavy electron component in Kondo lattice materials is the anisotropy of the Knight shift anomaly. For example, in CeCoIn₅ the Knight shift of the In(1) site exhibits a strong anomaly for $\mathbf{H}_0 \parallel c$ but no anomaly for $\mathbf{H}_0 \perp c$ [21]. In order to probe this behavior in greater detail, we have measured the full Knight shift tensor in CeIrIn₅. CeIrIn₅ is isostructural to CeCoIn₅, and is a superconductor with $T_c = 0.4$ K. A single crystal grown in In flux was mounted in a custom-made goniometer probe, and the orientation of the c -axis of the crystal was varied from 0 to 90 degrees. ¹¹⁵In has spin $I = \frac{9}{2}$, and there are two different crystallographic sites for In in this material; consequently there are several different transitions as seen in Fig. 5. Spectra were obtained as a function of orientation and temperature, and the Knight shift was extracted after correcting for the quadrupolar shift of the resonance [22]. Fig. 4 shows K versus θ , where θ is the angle between c and \mathbf{H}_0 .

The strong angular dependence can be understood in terms of the tensor nature of the hyperfine coupling. For $T > T^*$ the tensor is given by:

$$\mathbf{B} = \begin{pmatrix} B_{aa} & B_{ab} & B_{ac} \\ B_{ab} & B_{bb} & B_{bc} \\ B_{ac} & B_{bc} & B_{cc} \end{pmatrix} \quad [10]$$

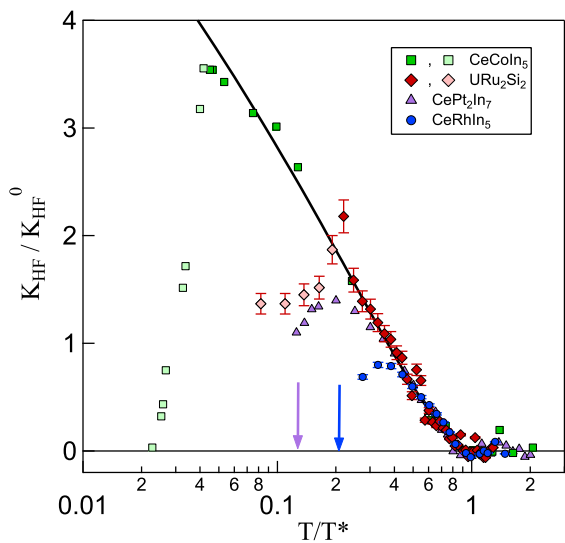


Fig. 13. $K_{HF}(T)$ (normalized) versus T/T^* for CeCoIn₅, CePt₂In₇, URu₂Si₂, and CeRhIn₅. Data points in the superconducting and hidden order states are lighter shades. The solid black line is Eq. 9, and the vertical arrows indicate T_N for CePt₂In₇ and CeRhIn₅. Data for the CeCoIn₅ and CePt₂In₇ are reproduced from Refs. [13] and [12].

in the basis defined by the tetragonal unit cell defined by the unit vectors a and c , and the susceptibility tensor is:

$$\chi = \begin{pmatrix} \chi_{aa} & 0 & 0 \\ 0 & \chi_{aa} & 0 \\ 0 & 0 & \chi_{cc} \end{pmatrix}. \quad [11]$$

We therefore have:

$$K(\theta) = K_{aa} \sin^2 \theta + K_{cc} \cos^2 \theta + K_{ac} \sin \theta \cos \theta \quad [12]$$

where θ is the angle between \mathbf{H}_0 and the c -axis, $K_{aa} = K_{aa}^0 + B_{aa}\chi_{aa}$, $K_{cc} = K_{cc}^0 + B_{cc}\chi_{cc}$, and $K_{ac} = K_{ac}^0 + B_{ac}(\chi_{aa} + \chi_{cc})$. The solid lines in Fig. 4(a) are fits to this equation, and Fig. 4(b) shows K_{aa} , K_{cc} and K_{ac} versus χ_{aa} , χ_{cc} and $\chi_{aa} + \chi_{cc}$, respectively. The fitted values are given in Table 2. The solid lines are fits that yield the hyperfine couplings B_{aa} , B_{cc} , B_{ac} and the orbital shifts K_{aa}^0 , K_{cc}^0 and K_{ac}^0 . The fact that $B_{ac} \approx 0$ within error bars implies that the principal axes of the hyperfine tensor coincide with those of the unit cell. On the other hand, $K_{ac}^0 \neq 0$ implies that the orbital shift tensor is not diagonal in the crystal basis. Rather it is rotated by an angle of $\sim 28^\circ$ from the c -direction, suggesting a possible role of directionality between the In 5p orbitals and the Ce 4f orbitals.

The emergence of the heavy fermion fluid is evident by computing $K_{HF}(\theta, T) = K(\theta, T) - K(\theta)$, where $K(\theta)$ is given by Eq. 12 and using the fitted parameters. This data is shown in Fig. 6, as well as fits to Eq. 9, which give a value of $T^* = 31(5)$ K. From this data, it is clear that T^* does not vary as a function of angle, but rather the overall scale of the quantity K_{HF}^0 decreases with angle until it reaches approximately zero by $\theta = 90^\circ$. The angular dependence clearly indicates that $K_{HF}(\theta, T)$ does not simply vanish for the perpendicular direction, but decreases gradually as a function of orientation in a continuous fashion. The constant K_{HF}^0 is anisotropic, but T^* is not. In fact, \mathbf{K}_{HF}^0 is proportional to $\mathbf{A} - \mathbf{B}$, and is therefore a tensor quantity itself, which is clearly seen in the angular dependence shown in the inset of Fig. 6. The solid line is a fit to $K_{HF}^0 = K_{HF,c}^0 \cos^2 \theta + K_{HF,a}^0 \sin^2 \theta$. It is likely that the anisotropy arises primarily because of the hyperfine couplings, but it is not possible to rule out an additional contribution to the anisotropy from the quantity $\chi_{cf} + \chi_{cc}$. The fact that T^* does not depend on orientation suggests that the field \mathbf{H}_0 has little effect on the onset of coherence.

Superconducting order

A key question in Kondo lattice materials is how the emergent heavy electron fluid and the remaining local moments interact to give rise to long range ordered states. Several materials exhibit a superconducting ground state, and it has long been assumed that the condensate forms from heavy electron quasiparticles. Recently we showed that this interpretation is supported by direct measurements of the Knight shift in the superconducting state [12]. Fig. 7 displays $K(T)$ and $K_{HF}(T)$ for the In and Co sites in CeCoIn₅. Surprisingly, the total Knight shift $K(T)$ *increases* for some of the sites below T_c , and decreases for others. The normal expectation is that the spin susceptibility decreases below T_c in a superconductor because the Cooper pairs have zero spin. Application of the two fluid analysis indicates that the heavy electron component, $K_{HF}(T)$, decreases as expected for a superconducting condensate. In fact, the data are best fit to a d-wave gap with value $\Delta(0) = 4.5k_B T_c$, in agreement with specific heat measurements. These results strongly suggest that the superconducting condensate arises as an instability of the heavy electron fluid.

Hidden order

Another well known heavy fermion system with long range order at low temperature is URu₂Si₂, which exhibits a phase transition to a state with an unknown order parameter at $T_{HO} = 17.5$ K [23]. This unusual phase has been studied for the past two decades and numerous theoretical order parameters have been proposed. Although the nature of the hidden order parameter remains unknown, extensive work has suggested that it has an itinerant nature and involves some type of Fermi surface instability [24]. We have measured the Knight shift of the ²⁹Si in URu₂Si₂ in order to investigate the effect of hidden order on K_{HF} .

Polycrystalline samples of URu₂Si₂ were synthesized by arc-melting in a gettered argon atmosphere, and an aligned powder was prepared in an epoxy matrix by curing a mixture of powder and epoxy in an external magnetic field of 9 T. Aligned powder samples are useful to enhance the surface-to-volume ratio and hence the NMR sensitivity. NMR measurements were carried out using a high homogeneity 500MHz (11.7T) Oxford Instruments magnet. The ²⁹Si($I = 1/2$) (natural abundance 4.6%) spectra were measured by spin echoes, and the signal-to-noise ratio was enhanced by summing several (~ 100) echoes acquired via a Carr-Purcell-Meiboom-Gill pulse sequence [25]. In this field, the hidden order transition is suppressed to 16 K [26]. The spin lattice relaxation rate (T_1^{-1}) was measured as a function of the angle between the alignment axis and the magnetic field \mathbf{H}_0 in order to properly align the sample, since T_1^{-1} is a strong function of orientation with a minimum for $\mathbf{H}_0 \parallel c$. Spectra are shown in Fig. 8, and the Knight shift along the c -direction, K_c , is shown in Fig. 9. The total magnetic susceptibility, $\chi_c(T)$, is shown in Figs. 8 and 9 as a solid line. χ_c exhibited little or no field dependence in the temperature range of interest. The inset of Fig. 9 displays K_c versus χ . There is a clear anomaly that develops around 75 K, in agreement with previous data from Bernal. However, in contrast to previous measurements, we find that below T^* the Knight shift turns upwards rather than downwards [27].

In order to fit the Knight shift data and extract the temperature dependence of K_{HF} , we have fit both the K_c versus χ data and the K_{HF} versus T data simultaneously by minimizing the joint reduced $\chi^2(K_0, B, K_{HF}^0, T^*) = \chi_1^2(K_0, B) + \chi_2^2(K_{HF}^0, T^*)$. Individually, χ_1^2 and χ_2^2 provide the best fits to the two data sets, but since $K_{HF}(T)$ depends on K_0 and B , χ_2^2 is an implicit function of these fit parameters as well. The best fit is shown in the inset of Fig. 9. The fit parameters, listed in Table 2, are close to the values originally reported by Kohori [28]. $K_{HF}(T)$ is shown in Fig. 10, and the best fit to Eq. 9 yields $T^* = 73(5)$ K. The data clearly indicate that $K_{HF}(T)$ grows monotonically down to the hidden ordering temperature at 16 K and is well described by the Yang-Pines scaling formula.

Since the f -electrons in URu₂Si₂ are strongly hybridized at low temperatures, the Knight shift and the susceptibility recover a one-component picture below a delocalization temperature T_L [4]. This allows us to determine the values of K_0 , A and B . The susceptibility of the two components below T^* hence can be subtracted and the results are plotted in Fig. 11. The local component also follows the mean-field prediction for a hybridized spin liquid [4], $\chi_l \sim f_l/(T + T_l + f_l\theta)$, with $f_0 = 1.6$, $\theta = 175$ K given by the RKKY coupling and $T_l = 70$ K by local hybridization.

Below the hidden order transition temperature K_{HF} decreases dramatically and saturates at a value $\sim K_{HF}(T_{HO})/3$ at $T \sim 4$ K. This result suggests that, like the superconductivity in CeCoIn₅, the hidden order phase in URu₂Si₂ emerges

from the itinerant heavy electron quasiparticles and is not a phenomenon associated with local moment physics [29]. The partial suppression of K_{HF} is also consistent with specific heat measurements which indicate that $\sim 40\%$ of the Fermi surface remains ungapped below the hidden order transition [30]. Recent theoretical work has suggested the presence of a pseudogap in a range of 5-10 K above the hidden order transition [31]. If one neglects the single outlying data point at 16 K, then the data may indicate a subtle change of scaling below ~ 23 K. However we do not have sufficient precision to make any conclusive statements about the pseudogap.

The Knight shift anomaly K_{HF} below T_{HO} also follows the BCS prediction,

$$K_{anom}(T) - K_{anom}(0) \sim \int dE \left(-\frac{\partial f(E)}{\partial E} \right) N(E), \quad [13]$$

where $f(E)$ is the Fermi distribution function and $N(E) = |E|/\sqrt{E^2 - \Delta(T)^2}$ is the density of states. The gap function $\Delta(T)$ has a mean-field temperature dependence,

$$\Delta(T) = \Delta(0) \tanh \left[2\sqrt{(T_{HO}/T - 1)} \right], \quad [14]$$

where $\Delta(0) \sim 4.0k_B T_{HO}$ is the gap amplitude determined by STM experiments. We find a good fit to the Kondo liquid susceptibility below T_{HO} in Fig. 11.

Antiferromagnetism and Relocalization

In order to investigate the response of K_{HF} to long-range order we have measured the Knight shift of the $^{115}\text{In}(1)$ site in CeRhIn₅. CeRhIn₅ is an antiferromagnet at ambient pressure with an ordered moment of $0.4\mu_B$ and $T_N = 3.8\text{K}$ [32]. Single crystals were grown in In flux using standard flux growth techniques. The $\frac{3}{2} \leftrightarrow \frac{1}{2}$ transition of the ^{115}In ($I = 9/2$) was observed for the In(1) by Hahn echoes, and the alignment of the crystal was confirmed by the splitting of the quadrupolar satellites [33]. The Knight shift is shown in Fig. 12. There is a clear anomaly that develops at 17 K, in contrast to a previous report of 12 K [11]. In this case the previous data consisted of only six data points over a limited range and did not have the precision to discern the anomaly. By taking more data points at closely spaced intervals, we find K_c increases above the extrapolated value below T^* , in contrast to that in the CeIrIn₅ and CeCoIn₅ (see Fig. 1). The best fits to the data yield hyperfine couplings that are similar to those in CeIrIn₅ (see Table 2), and we find that $T^* = 18(1)\text{ K}$ for CeRhIn₅.

The temperature dependence of the emergent heavy fermion component, $K_{HF}(T)$ is shown in Fig. 10(b) for CeRhIn₅. In contrast to the scaling behavior observed in CeIrIn₅, CeCoIn₅ and URu₂Si₂, K_{HF} does not follow the Yang-Pines scaling formula down to the ordering temperature, T_N . Rather, K_{HF} begins to deviate below 9 K, exhibits a maximum at 8 K and then decreases down to T_N . This temperature of the breakdown of scaling corresponds well with the onset of antiferromagnetic correlations observed by inelastic neutron scattering and NMR spin lattice relaxation measurements [34, 35]. The physical picture that emerges is that the local moments begin to hybridize below T^* , but their spectral weight is only gradually transferred to the heavy electron fluid. At 9 K, the partially screened local moments begin to interact with one another and spectral weight is transferred back. This *relocalization* behavior was first observed in the antiferromagnet CePt₂In₇ [13]. The fact that K_{HF} remains finite at T_N suggests that the ordered local moments still remain partially screened [4].

It is interesting to compare the behavior of the heavy electron Knight shift observed in URu₂Si₂ and CeRhIn₅ with other Kondo lattice materials that undergo long range order. Fig. 13 shows the scaled K_{HF} versus T/T^* for URu₂Si₂, CeRhIn₅, CeCoIn₅, and the antiferromagnet CePt₂In₇ ($T_N = 5.2\text{ K}$, $T^* \approx 40\text{ K}$) [11, 13]. The onset of hybridization at T^* is identical for all the compounds, but the low temperature behavior depends critically on the ground state. In both CeCoIn₅ and URu₂Si₂ the spectral weight appears to be transferred continuously to the heavy electron fluid all the way down to the ordering temperature. Similar behavior is present in CeIrIn₅ ($T_c = 0.4\text{ K}$, not shown) down to 2 K. This behavior is surprising, because one might expect that the hidden order and/or superconductivity would emerge from a fully formed heavy electron state. Such a state would be characterized by a temperature independent K_{HF} , but that is clearly not the case for either material. In fact, the only known cases where K_{HF} appears to plateau at a constant value are CeSn₃ and Ce₃Bi₄Pt₃, neither of which exhibit long range order [11].

The relocalization behavior in CeRhIn₅ and CePt₂In₇ contrasts starkly with that of the URu₂Si₂ and CeCoIn₅, where K_{HF} exhibits a peak in the paramagnetic state. In CePt₂In₇ K_{HF} was determined via ¹⁹⁵Pt NMR in a powder sample, thus the precision was not as high as for a single crystal in which the full susceptibility tensor can be measured [13]. The new results in the CeRhIn₅ reported here, however, were indeed acquired in a single crystal and confirm that relocalization behavior appears to be a common feature of antiferromagnetic materials.

Conclusions

We have measured the emergence of the Kondo liquid and investigated its response to long range order in several heavy fermion compounds. In the superconductors CeCoIn₅ and CeIrIn₅ as well as the hidden order compound URu₂Si₂, K_{HF} rises continuously below T^* down to the ordering temperature without saturation. In the antiferromagnets CeRhIn₅ and CePt₂In₇ the Kondo liquid relocalizes as a precursor to long range order or partially screened local moments. Much of this behavior can be understood in the framework of *hybridization effectiveness* introduced in the context of the two-fluid phenomenology [4]. In this picture $K_{HF}(T) \sim f_0$, where f_0 is a measure of the collective hybridization that reduces the magnitude of the local f -moments, and $f_0 = 1$ corresponds to complete hybridization. CeCoIn₅, CeIrIn₅ and URu₂Si₂ correspond to materials with $f_0 > 1$, whereas CeRhIn₅ and CePt₂In₇ have $f_0 < 1$. Although the results reported here do not directly address issues of non-Fermi liquid behavior and the presence of quantum critical phenomena in Kondo lattice systems, they do have important implications for theory [36, 37]. The dual nature of the coexisting local moments and the heavy electron fluid that exists in these materials below T^* suggests that the physics cannot be described in terms of a single electronic degree of freedom. Rather, the interactions between the local moments, the heavy electron quasiparticles, and their relative spectral weight should be taken into account.

ACKNOWLEDGMENTS. We thank S. Balatsky, P. Coleman, M. Graf, D. Pines and J. Thompson for stimulating discussions. Work at UC Davis was supported by UCOP-TR01, the National Nuclear Security Administration under the Stewardship Science Academic Alliances program through DOE Research Grant #DOE DE-FG52-09NA29464, and the National Science Foundation under Grant No. DMR-1005393. Work in China was supported by the Chinese Academy of Sciences and NSF-China (Grant No. 11174339). Los Alamos National Laboratory is operated by Los Alamos National Security, LLC, for the National Nuclear Security Administration of the US Department of Energy under Contract No. DE-AC52-06NA25396.

1. Löhneysen, H. v., Rosch, A., Vojta, M. & Wölfle, P. Fermi-liquid instabilities at magnetic quantum phase transitions. *Rev. Mod. Phys.* **79**, 1015–1075 (2007).
2. Doniach, S. The kondo lattice and weak antiferromagnetism. *Physica* **91B**, 231–234 (1977).
3. Yang, Y.-F., Fisk, Z., Lee, H.-O., Thompson, J. D. & Pines, D. Scaling the kondo lattice. *Nature* **454**, 611 (2008).
4. Yang, Y.-F. & Pines, D. Emergent states in heavy electron materials. *Proceedings of the National Academy of Sciences* ??, ?? (2012).
5. Yamamoto, S. J. & Si, Q. Fermi surface and antiferromagnetism in the kondo lattice: An asymptotically exact solution in $d \geq 1$ dimensions. *Phys. Rev. Lett.* **99**, 016401 (2007).
6. Custers, J., Gegenwart, P., Wilhelm, H., Neumaier, K., Tokiwa, Y., Trovarelli, O., Geibel, C., Steglich, F., Pepin, C. & Coleman, P. The break-up of heavy electrons at a quantum critical point. *Nature* **424**, 524 (2003).
7. Stockert, O. et al. Nature of the α phase in CeCu_2Si_2 . *Phys. Rev. Lett.* **92**, 136401 (2004).
8. Park, T., Graf, M. J., Boulaevskii, L., Sarrao, J. L. & Thompson, J. D. Electronic duality in strongly correlated matter. *Proc. Natl. Acad. Sci.* **105**, 6825–6828 (2008). <http://www.pnas.org/content/105/19/6825.full.pdf+html>.
9. Nakatsuji, S., Pines, D. & Fisk, Z. Two fluid description of the kondo lattice. *Phys. Rev. Lett.* **92**, 016401 – 4 (2004).
10. Yang, Y.-F. & Pines, D. Universal behavior in heavy-electron materials. *Phys. Rev. Lett.* **100**, 096404 (2008).
11. Curro, N. J., Young, B. L., Schmalian, J. & Pines, D. Scaling in the emergent behavior of heavy-electron materials. *Phys. Rev. B* **70**, 235117 – 1 (2004).
12. Yang, Y.-F., Urbano, R., Curro, N. J., Pines, D. & Bauer, E. D. Magnetic excitations in the kondo liquid: Superconductivity and hidden magnetic quantum critical fluctuations. *Phys. Rev. Lett.* **103**, 197004 (2009).
13. apRoberts Warren, N., Dioguardi, A. P., Shockley, A. C., Lin, C. H., Crocker, J., Klavins, P., Pines, D., Yang, Y.-F. & Curro, N. J. Kondo liquid emergence and re-localization in the approach to antiferromagnetic ordering in CePt_2In_7 . *Phys. Rev. B* **83**, 060408 (2011).
14. Clogston, A. M. & Jaccarino, V. Susceptibilities and negative knight shifts of intermetallic compounds. *Phys. Rev.* **121**, 1357–1362 (1961).
15. Abragam, A. *The Principles of Nuclear Magnetism* (Oxford University Press, Oxford, 1961).
16. Kim, E., Makivic, M. & Cox, D. L. Knight shift anomalies in heavy electron materials. *Phys. Rev. Lett.* **75**, 2015–2018 (1995).
17. Ohama, T., Yasuoka, H., Mandrus, D., Fisk, Z. & Smith, J. L. Anomalous transferred hyperfine coupling in CeCu_2Si_2 . *J. Phys. Soc. Jpn.* **64**, 2628 (1995).
18. Mila, F. & Rice, T. M. Spin dynamics of $\text{YBa}_2\text{Cu}_3\text{O}_{6+x}$ as revealed by nmr. *Phys. Rev. B* **40**, 11382–11385 (1989).
19. Christianson, A. D. et al. Crystalline electric field effects in CeIn_5 ($m = \text{Co, Rh, Ir}$): superconductivity and the influence of kondo spin fluctuations. *Phys. Rev. B* **70**, 134505 (2004).
20. Curro, N. J. Nuclear magnetic resonance in the heavy fermion superconductors. *Rep. Prog. Phys.* **72**, 026502 (24pp) (2009).
21. Curro, N. J., Simovic, B., Hammel, P. C., Pagliuso, P. G., Sarrao, J. L., Thompson, J. D. & Martins, G. B. Anomalous nmr magnetic shifts in CeCoIn_5 . *Phys. Rev. B* **64**, 180514 – 4 (2001).
22. Curro, N. J. *Encyclopedia of Magnetic Resonance*, chap. Quadrupolar NMR of Superconductors (John Wiley: Chichester, 2011).
23. Mydosh, J. A. & Oppeneer, P. M. Colloquium : Hidden order, superconductivity, and magnetism: The unsolved case of Uru_2Si_2 . *Rev. Mod. Phys.* **83**, 1301–1322 (2011).
24. Wiebe, C. R. et al. Gapped itinerant spin excitations account for missing entropy in the hidden-order state of Uru_2Si_2 . *Nat. Phys.* **3**, 96–99 (2007).
25. Slichter, C. P. *Principles of Nuclear Magnetic Resonance* (Springer-Verlag, 1992), 3rd edn.
26. Harrison, N., Jaime, M. & Mydosh, J. A. Reentrant hidden order at a metamagnetic quantum critical end point. *Phys. Rev. Lett.* **90**, 096402 (2003).
27. Bernal, O., Becker, B., Mydosh, J., Nieuwenhuys, G., Menovsk, A., Paulus, P., Brom, H., MacLaughlin, D. & Lukefahr, H. Nmr detection of temperature-dependent magnetic inhomogeneities in Uru_2Si_2 . *Physica B: Condensed Matter* **281 – 282**, 236 – 237 (2000).
28. Kohori, Y., Matsuda, K. & Kohara, T. ^{29}Si nmr study of antiferromagnetic superconductor Uru_2Si_2 . *J. Phys. Soc. Jpn.* **65**, 1083 – 1086 (1996).
29. Hanzawa, K. Hidden octupole order in Uru_2Si_2 . *J. Phys.: Condens. Matter* **19**, 072202 (2007).
30. Maple, M. B., Chen, J. W., Dalichaouch, Y., Kohara, T., Rossel, C., Torikachvili, M. S., McElfresh, M. W. & Thompson, J. D. Partially gapped fermi surface in the heavy-electron superconductor Uru_2Si_2 . *Phys. Rev. Lett.* **56**, 185–188 (1986).
31. Haraldsen, J. T., Dubi, Y., Curro, N. J. & Balatsky, A. V. Hidden-order pseudogap in Uru_2Si_2 . *Phys. Rev. B* **84**, 214410 (2011).
32. Llobet, A. et al. Magnetic structure of CeRhIn_5 as a function of pressure and temperature. *Phys. Rev. B* **69**, 24403 – 1 (2004).
33. Hegger, H., Petrovic, C., Moshopoulou, E. G., Hundley, M. F., Sarrao, J. L., Fisk, Z. & Thompson, J. D. Pressure-induced superconductivity in quasi-2d CeRhIn_5 . *Phys. Rev. Lett.* **84**, 4986–4989 (2000).
34. Bao, W., Pagliuso, P. G., Sarrao, J. L., Thompson, J. D., Fisk, Z., Lynn, J. W. & Erwin, R. W. Incommensurate magnetic structure of CeRhIn_5 . *Phys. Rev. B* **62**, R14621 – 4 (2000).
35. Curro, N. J., Sarrao, J. L., Thompson, J. D., Pagliuso, P. G., Kos, S., Abanov, A. & Pines, D. Low-frequency spin dynamics in the CeIn_5 materials. *Phys. Rev. Lett.* **90**, 227202 – 4 (2003).
36. Si, Q. M., Rabello, S., Ingersent, K. & Smith, J. L. Locally critical quantum phase transitions in strongly correlated metals. *Nature* **413**, 804 – 808 (2001).
37. Coleman, P. & Schofield, A. J. Quantum criticality. *Nature* **433**, 226 – 9 (2005).

Table 1. Crystal Field Levels and Coherence Temperatures in the CeMIn₅ Materials

Material	T^* (K)	Δ (K)(from [19])
CeCoIn ₅	42	100
CeRhIn ₅	18(1)	80
CeIrIn ₅	31(5)	78

Table 2. Measured hyperfine coupling constants in CeIrIn₅, CeRhIn₅ and URu₂Si₂

Material	site	B_{aa} (kOe/ μ_B)	B_{cc} (kOe/ μ_B)	B_{ac} (kOe/ μ_B)	K_{aa}^0 (%)	K_{cc}^0 (%)	K_{ac}^0 (%)
CeIrIn ₅	In(1)	11.3(1)	13.8(1)	0.4(3)	1.1(2)	0.4(2)	-0.5(2)
CeRhIn ₅	In(1)	—	21.4(5)	—	—	0.64(5)	—
URu ₂ Si ₂	Si	—	4.3(1)	—	—	-0.07(1)	—